



ARTICLE

A Novel Bio-Based Zirconium Phosphonate as a Flame Retardant and Smoke Suppressant for Epoxy Resin

Xianling Fu[#], Hongliang Ding[#], Xin Wang^{*}, Lei Song and Yuan Hu^{*}

State Key Laboratory of Fire Science, University of Science and Technology of China, Hefei, 230026, China

^{*}Corresponding Authors: Xin Wang. Email: wxcmx@ustc.edu.cn; Yuan Hu. Email: yuanhu@ustc.edu.cn

[#]These authors contributed equally to this paper

Received: 10 December 2021 Accepted: 17 January 2022

ABSTRACT

Although epoxy resin has been widely used in various fields, it still suffers from some problems including brittleness and flammability. In this study, a new phosphonic acid, N, N-bis(phosphomethyl) glycine (GDMP), was prepared by Mannich reaction with bio-based glycine and then a novel layered zirconium phosphonate (ZrGDMP) was synthesized using GDMP and zirconyl chloride hydrate as reactants. The chemical structure of ZrGDMP was well characterized by ¹H and ³¹P NMR, SEM, XRD and XPS. The effect of ZrGDMP on the flame retardancy, smoke suppression, strengthening and toughening performances of the epoxy matrix was investigated and evaluated. TGA results indicated that compared with pure EP, ZrGDMP-EP composites showed higher char yield due to the catalytic charring effect of ZrGDMP. The pure EP exhibited high flammability, while ZrGDMP-EP composites possessed excellent thermal stability and remarkable fire resistance. The PHRR, THR, and TSP values of 3wt% ZrGDMP-EP were obviously declined by 39.6%, 40.2%, and 24.9% compared to these of pure EP. Moreover, the tensile and impact tests implied that the addition of ZrGDMP can significantly reinforce the toughness as well as the strength of EP in terms of higher impact strength (24.8 kJ/m²) and tensile strength (57.7 MPa), which was mainly contributed to the uniform dispersion of ZrGDMP within the EP matrix.

KEYWORDS

Zirconium phosphonate; epoxy resin; flame retardant; mechanical property

1 Introduction

As one of the most common commercial polymer materials, epoxy resin possesses various excellent comprehensive properties including light quality, corrosion resistance, excellent adhesion, low dielectric constant, dielectric and superior adhesion property [1–3]. Therefore, it has wide applications in many high-tech fields such as construction, aerospace, coating and integrated circuits throughout the national economic life [4,5]. Although epoxy resin has many excellent properties, it still has a common problem like other commercial polymer materials: flammability [6,7]. Moreover, after the curing process, the cross-linking density of EP is high, which endows EP with high strength, but EP suffers from brittleness and is easy to break. It is necessary to endow EP with excellent flame retardancy and mechanical properties [8,9]. Generally, the most widely used method is to add some flame retardant to improve the flammability of polymers, which is convenient and easy to conduct [10,11]. However, it will affect other



properties of polymer materials such as the worseness of mechanical property if too much flame retardant is added to the matrix. Because it is easy to agglomerate in the matrix, the research about additive flame retardant focus on the flame retardant efficiency and dispersion state of additive flame retardant in the matrix [12,13]. It has been proved that well-dispersed inorganic nanoparticles can enhance the mechanical properties of polymers, while organic molecules serve as a small molecular plasticizer and toughen the polymer materials [14].

Zirconium phosphate (ZrP) is one kind of solid acid with a nano-layered structure, which can catalyze the char formation of polymers and show remarkable flame retardant and smoke suppression effects [15,16]. As an inorganic material, zirconium phosphate exhibits poor interface compatibility with polymer matrix and is easy to aggregate in the matrix [17–19]. The organic zirconium phosphonate synthesized by organic phosphonic acid not only has a nanostructure and acid catalysis similar to that of inorganic zirconium phosphate but also contains organic components with larger volumes [20]. Due to the existence of hydroxyl groups between the inorganic zirconium phosphate sheets, sheets are interacted with each other by hydrogen bond [21]. There are organic components between the organic zirconium phosphonate sheets, resulting in a small interaction force between nanosheets. The volume of organic molecular is larger than the hydroxyl group so that the interlayer spacing of organic zirconium phosphonate is larger than that of inorganic zirconium phosphate. If the interlayer spacing of the layered compound is larger, it will be dispersed better in the matrix. Thus, compared with inorganic zirconium phosphate, organic zirconium phosphonate possesses better interface compatibility with matrix so that it can be evenly dispersed in the EP matrix, and has multiple enhancement effects of flame retardant, smoke suppression and toughness on EP [22–24].

In recent years, with the increasing concerns on environmental pollution, the development of flame retardant additives from bio-based resources has aroused extensive research enthusiasm. Glycine, also known as aminoacetic acid, is a non-essential amino acid, which comes from high protein foods such as milk, beans and cheese. Hence, in this work, glycine was selected to synthesize a novel bio-based zirconium phosphonate (ZrGDMP). XRD and XPS were utilized to characterize the chemical structure of ZrGDMP. The effect of ZrGDMP on the comprehensive properties of epoxy resins was also investigated, including the thermal stability, fire resistance performance, and mechanical property. It is expected that the simple strategy can guide the development of the novel hybrid flame retardants.

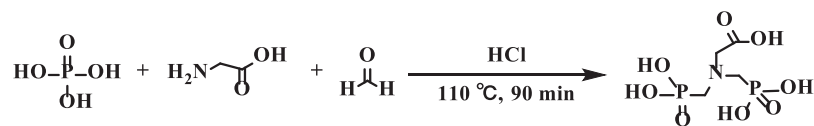
2 Experiment

2.1 Materials

Glycine, formaldehyde solution (37.0%–40.0%), hydrofluoric acid (concentration $\geq 40\%$ in H_2O) and 4,4'-diamino-diphenylmethane (DDM) were bought from Sinophenol Chemical Reagent Co., Ltd. (Shanghai, China). Solid phosphite, zirconyl chloride hydrate ($ZrOCl_2 \cdot 8H_2O$) and phenylphosphonic were obtained from Aladdin Chemical Reagent Co., Ltd. (Shanghai, China). Diglycidyl ether bisphenol A epoxy resin (DGEBA) was offered by Hefei Jiangfeng Chemical Co., Ltd. (Hefei, China).

2.2 Synthesis of *N, N*-bis (Phosphonomethyl) Glycine (GDMP)

50 mL deionized water, 10 mL concentrated hydrochloric acid, 40.1 g (0.5 mol) phosphite, and 18.76 g (0.25 mol) glycine were added successively into a 250 mL three-necked flask and dissolved by magnetic stirring. Subsequently, the mixed solution was heated to $95^\circ C$ in the oil bath and 61.4 g (0.75 mol) formaldehyde solution was dripped into the mixed solution by a dripping funnel in 10–15min. The solution was heated to $110^\circ C$ and refluxed for 90 min. After cooling down, the product GDMP was the white substance precipitated from the acetone solution. The synthesis of GDMP is shown in [Scheme 1](#).



Scheme 1: The synthesis of GDMP

2.3 Synthesis of *N, N*-bis (Phosphonic Acid Methyl) Glycine Zirconium Phosphonate (ZrGDMP)

400 mL deionized water, 30 g HF solution and 32.2 g (0.1 mol) zirconium oxychloride were added into a 500 mL beaker, then dissolving by magnetic stirring on a magnetic agitator. 20.37 g (0.1 mol) of GDMP was dissolved in 100 mL deionized water and then added to the beaker by using the dropping funnel. After dropping all, the beaker was moved to an oven at 80°C for 48 h. After centrifugation at 10,000 rpm for 5 min, the supernatant was washed until the pH was over 5 and then dried in an oven at 60°C. The structure of ZrGDMP is presented in Fig. 1.

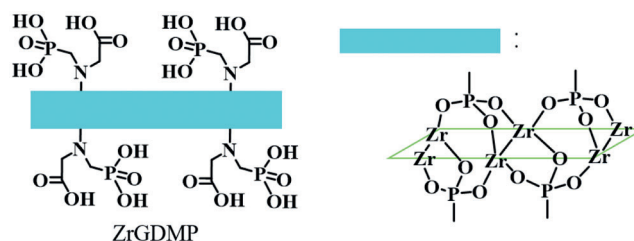


Figure 1: The structure of ZrGDMP

2.4 Preparation of ZrGDMP-EP Composites

ZrGDMP-EP composite materials with different ZrGDMP content were prepared. Taking the preparation process of 2wt% ZrGDMP-EP as an example, 2 g ZrGDMP was dispersed in 30 mL acetone, then the solution was mechanically stirred and ultrasonically treated for 30 min. The solution was mixed with 80.5 g epoxy resin for 1 h. After that, rotating evaporation was used to remove the solvent acetone at 60°C for another 1 h. Then, 17.5 g DDM was added to the mixture, stirring gently so that all the substances were uniformly mixed. Then the mixture was slowly poured into the mold prepared in advance and cured at 100°C for 2h, then cured at 150°C for 2 h. The prepared epoxy resin composites were named 0.5wt% ZrGDMP-EP, 1wt% ZrGDMP-EP, 2wt% ZrGDMP-EP and 3wt% ZrGDMP-EP.

2.5 Characterization

The ¹H and ³¹P Nuclear Magnetic Resonance (NMR) were carried out on the Bruker AVANCE-400NMR spectrometer, which used D₂O as the solvent and operated in Fourier transform mode.

X-ray diffraction (XRD) patterns were measured by a PHILIPS X'PERT-PRO spectrometer. The test data was collected by a step scanning procedure.

The morphology of ZrGDMP nanosheets and char residue was observed by JEOL JSM-6700F scanning electron microscope (SEM) with a voltage of 10 kV.

Thermo ESCALAB 250Xi X-ray photoelectron spectroscopy (XPS) was used to study the elemental composition of ZrPP.

The thermogravimetric analysis (TGA) of EP composites was measured by the TAQ5000 thermal analyzer under air and N₂ atmosphere at a heating rate of 20 °C/min from 25°C to 800°C.

The flame retardant behavior of epoxy composites was determined by an FTT cone calorimeter following ISO 5660-1 procedure. The dimension size of all samples was 100 mm × 100 mm × 3 mm. After mounting in aluminum foil, the sample was horizontally exposed to a heat flux of 50 kW/m².

PerkinElmer STA8000 thermogravimetric analyzer was used for thermogravimetric analysis-Fourier transform infrared spectrometry (TG-FTIR), which was connected with the PerkinElmer Frontier FT-IR spectrometer at a heating rate of 20 °C/min under N₂ atmosphere.

Raman spectroscopy (Raman) was conducted on Laser Confocal Raman Microscope (LabRAM HR Evolution, France) with tested wavenumbers starting from 500 to 2000 cm⁻¹.

The limiting oxygen index (LOI) of the specimens was tested on the HC-2 oxygen index analyzer (Jiangning, China) according to the GB/T 2406.2-2009 standard.

The tensile test was performed on an MTS criterion 43 electromechanical universal testing machine according to the ASTM D3039-08 standard. The ZBC1400-A pendulum impact testing machine (MTS Company of China) was prepared for the impact test according to the GB/T 1043.1-2008 standard. The size of all samples for the tensile test and impact test was 100 mm × 10 mm × 4 mm.

3 Results and Discussion

3.1 Structural and Morphological Characterization

The ¹H and ³¹P spectra of GDMP are shown in Figs. 2a and 2b. Due to the high polarity of GDMP, the active H was replaced by deuterium, so the signal of -OH of GDMP was not observed in ¹H NMR spectrum. The signal at 3.53 ppm corresponded to the methylene near the phosphate group, while the peak at 4.25 ppm was ascribed to the methylene near the carboxyl group. The signal peak at 4.76 ppm was the water peak. As shown in ³¹P NMR spectra, there was only one peak at 7.60 ppm, indicating that GDMP was successfully synthesized. Figs. 2c and 2d provide the SEM images of ZrGDMP. It can be seen that the synthesized ZrGDMP was flaky and the size was not very uniform, while some of them were long flakes. The width of small nanosheets was about 100 nm, but the length of long-strip nanosheets was about 500 nm. The surface of the sheet structure of ZrGDMP was smooth, indicating that the crystallinity of ZrGDMP was high. X-ray diffraction (XRD) pattern of ZrGDMP is presented in Fig. 2e. It was obviously seen that the reflection peak of the crystal plane (002) of ZrGDMP moved to 2θ = 7.2°, and the layer spacing of ZrGDMP was 1.227 nm, which was larger than that of ZrP (0.743 nm) [25,26]. Many organic groups such as phosphonic acid groups were bonded on the ZrGDMP layers, which weakened the intermolecular hydrogen bonding between the ZrGDMP sheets so that the distance between the layers was increased. The element composition and relative content of ZrGDMP were measured by XPS (Fig. 2f). ZrGDMP mainly contained C, O, N, Zr, and P, and their atom percentages were 29.08%, 45.56%, 6.93%, 4.21%, and 14.21%, respectively. The N element mainly came from glycine, which was used as the raw material for the synthesis of organic phosphonic acid.

3.2 Thermal Properties

The TGA and DTG curves of GDMP and ZrGDMP in the air and N₂ atmosphere are presented in Fig. 3, while the relevant data are shown in Table 1. It was obvious that both GDMP and ZrGDMP underwent two thermal degradation stages in the air or N₂ atmosphere. The char yield of GDMP was only 12.1 wt% and the T_{-5%} was just 166°C in the air atmosphere, which was not significantly different from that of GDMP in the N₂ atmosphere. But the T_{max2} was quite different in the two atmospheres, the T_{max2} in the air atmosphere was 630°C, which was much higher than that in the N₂ atmosphere (528°C). Compared with GDMP, ZrGDMP possessed higher thermal stability with less degradation loss and high char yield in air atmosphere about 83.7 wt%. However, both T_{max1} and T_{max2} of ZrGDMP were lower than GDMP, indicating the decomposition of ZrGDMP in advance during the heating process. The T_{max1} of ZrGDMP was only 127°C in the air atmosphere, which was quite lower than that in the N₂ atmosphere (243°C).

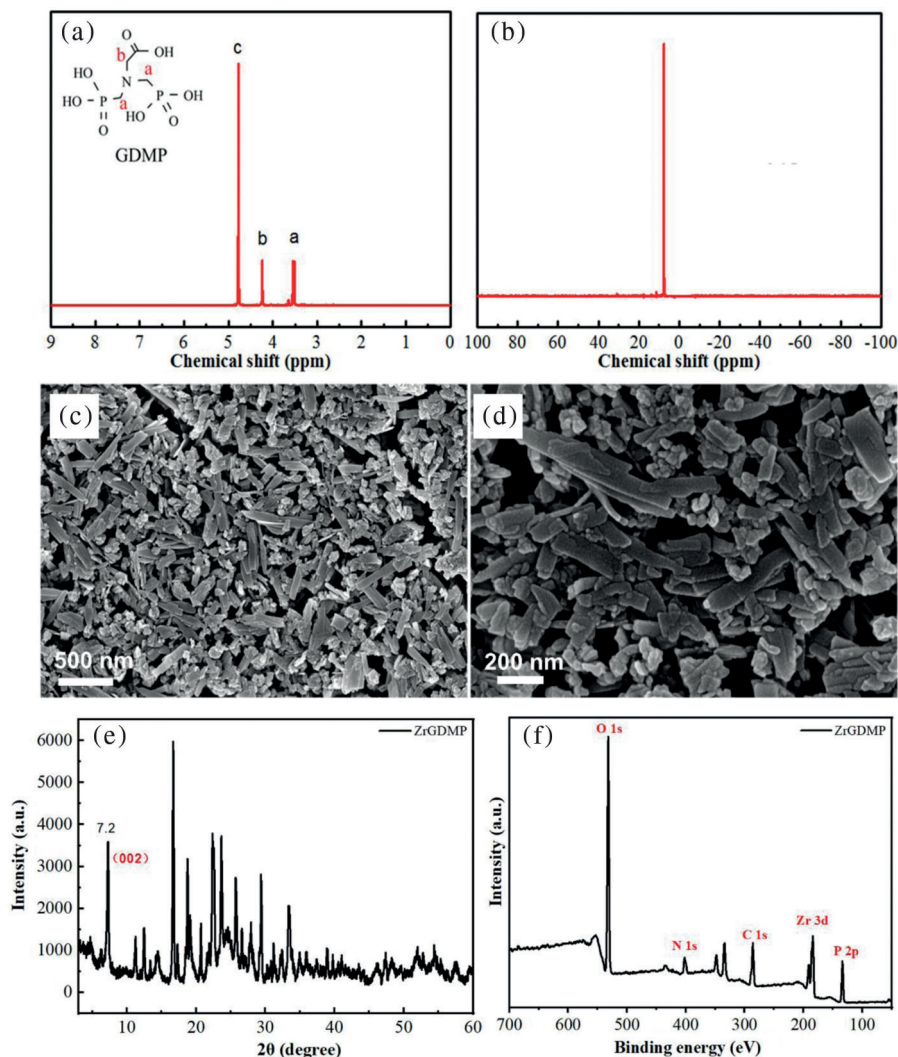


Figure 2: The (a) ^1H and (b) ^{31}P spectra of GDMP; (c) and (d) SEM images of the structure of ZrGDMP; (e) XRD pattern of ZrGDMP; (f) XPS survey spectrum of ZrGDMP

The TGA and DTG curves of EP and ZrGDMP-EP composites are shown in Fig. 4 and the TGA data of epoxy composites are summarized in Table 2. It can be seen that the pyrolysis curves of epoxy composites were consistent with that of pure EP, implying that the addition of ZrGDMP into EP did not affect the thermal degradation behavior of EP composites. Different from the pyrolysis behavior with two thermal degradation stages in the air atmosphere, all the composites showed only one thermal degradation stage in the N_2 atmosphere. In the N_2 atmosphere, all the composites degraded in advance, and the char yield of ZrGDMP-EP composites increased as well. However, in the air atmosphere, the pyrolysis temperature of epoxy resin composites did not change obviously compared with that of pure EP. No matter in the air or N_2 atmosphere, the char yield of the epoxy composite was increased, suggesting that the ZrGDMP nanosheets can promote the formation of char residue and inhibit the thermal degradation behavior of EP composites [27].

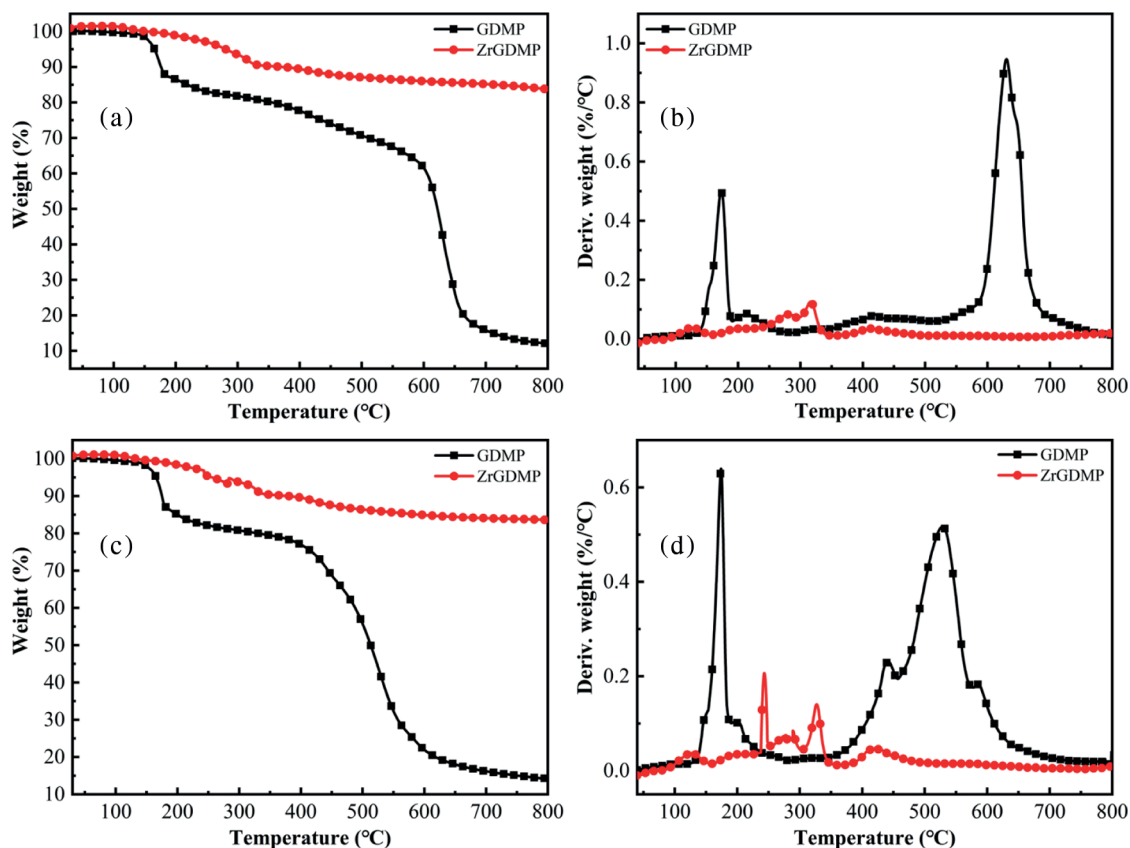


Figure 3: TGA and DTG curves of GDMP and ZrGDMP in (a, b) air and (c, d) N₂ atmospheres

Table 1: TGA data of GDMP and ZrGDMP in air and N₂ atmospheres

Sample	Air				N ₂			
	T _{-5%} (°C)	T _{max1} (°C)	T _{max2} (°C)	Char residue (wt%)	T _{-5%} (°C)	T _{max1} (°C)	T _{max2} (°C)	Char residue (wt%)
GDMP	166	173	630	12.1	165	174	528	14.1
ZrGDMP	281	127	316	83.7	256	243	327	83.6

3.3 Flame Retardant Properties

After incorporating with ZrGDMP, the LOI value of epoxy composites slightly increased from 25.0% to 28%. Cone calorimetry was further used to investigate the fire resistance performance of ZrGDMP-EP, which could provide several important parameters, including the peak heat release rate (PHRR), total heat release (THR), total smoke release (TSR) and CO production rate (COPR). HRR, THR, TSP and COPR curves of epoxy composites are presented in Fig. 5, whereas the detailed data are listed in Table 3. There was an obvious decrease of PHRR of epoxy composites after incorporating with ZrGDMP, and the PHRR of 3wt% ZrGDMP-EP was decreased by 39.6% from 1438 to 869 kW/m². The THR of 3wt% ZrGDMP-EP was notably decreased from 93.1 to 55.7 MJ/m². The significant decrease of PHRR and THR values of epoxy composites indicated that ZrGDMP can efficiently inhibit the heat release of EP. Similar to PHRR and THR, the TSP of ZrGDMP-EP composites was significantly reduced too, indicating the remarkable smoke suppression effect of ZrGDMP on EP composites. The peak value of COPR of epoxy composites

decreased to 0.020 g/s after adding only 0.5 wt% ZrGDMP, which was 48.1% lower than that of pure EP (0.039 g/s). The peak value of COPR of other composite materials with different ZrGDMP contents was similar to that of 0.5 wt% ZrGDMP. According to the results of the cone calorimeter, ZrGDMP possessed remarkable flame retardant and smoke suppression effects, which was mainly due to the higher phosphorus content and the synergistic flame retardant effect between phosphorus and nitrogen. In addition, ZrGDMP can catalyze the formation of the protective char layer which can serve as a physical barrier to suppress the smoke release and inhibit the heat transfer during combustion, resulting in lower TSP and COPR values.

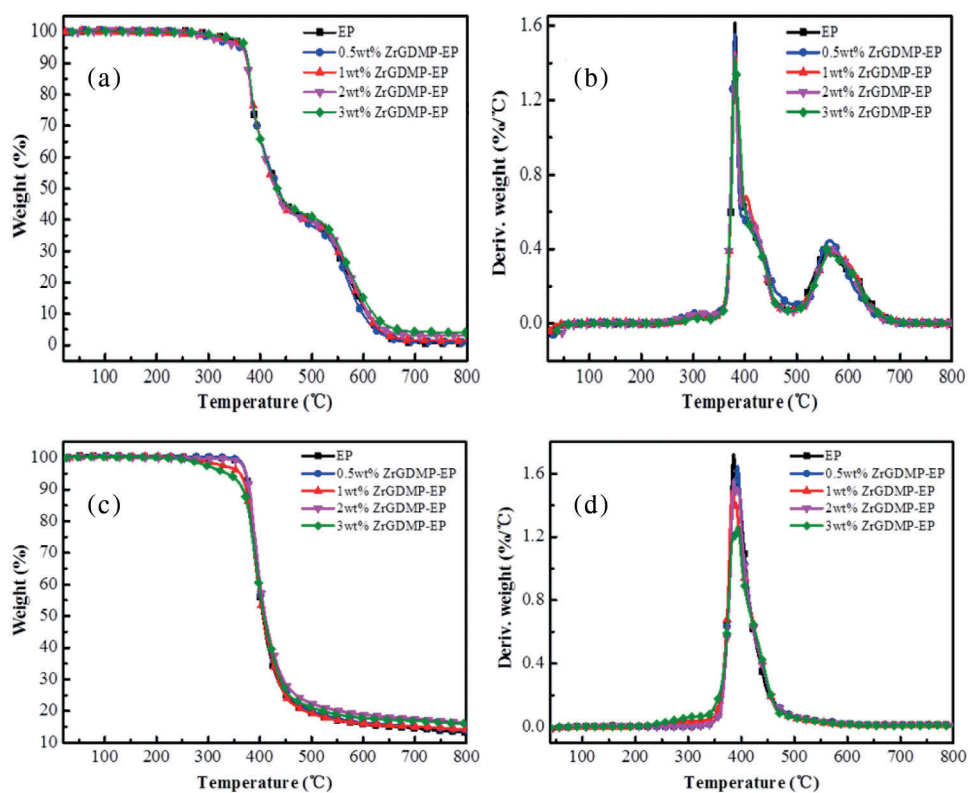


Figure 4: TGA and DTG curves of EP and ZrGDMP-EP composites in (a, b) air atmosphere and (c, d) N₂ atmospheres

Table 2: TGA data of EP and ZrGDMP-EP composites in air and N₂ atmospheres

Sample	Air				N ₂		
	T _{-5%} (°C)	T _{max1} (°C)	T _{max2} (°C)	Char residue (wt%)	T _{-5%} (°C)	T _{max} (°C)	Char residue (wt%)
EP	368	381	565	0.7	373	385	13.2
0.5wt% ZrGDMP-EP	363	381	563	0.9	373	392	13.9
1wt% ZrGDMP-EP	367	381	569	1.4	362	383	14.1
2wt% ZrGDMP-EP	363	380	569	3.1	373	386	16.2
3wt% ZrGDMP-EP	370	381	560	3.9	337	385	16.0

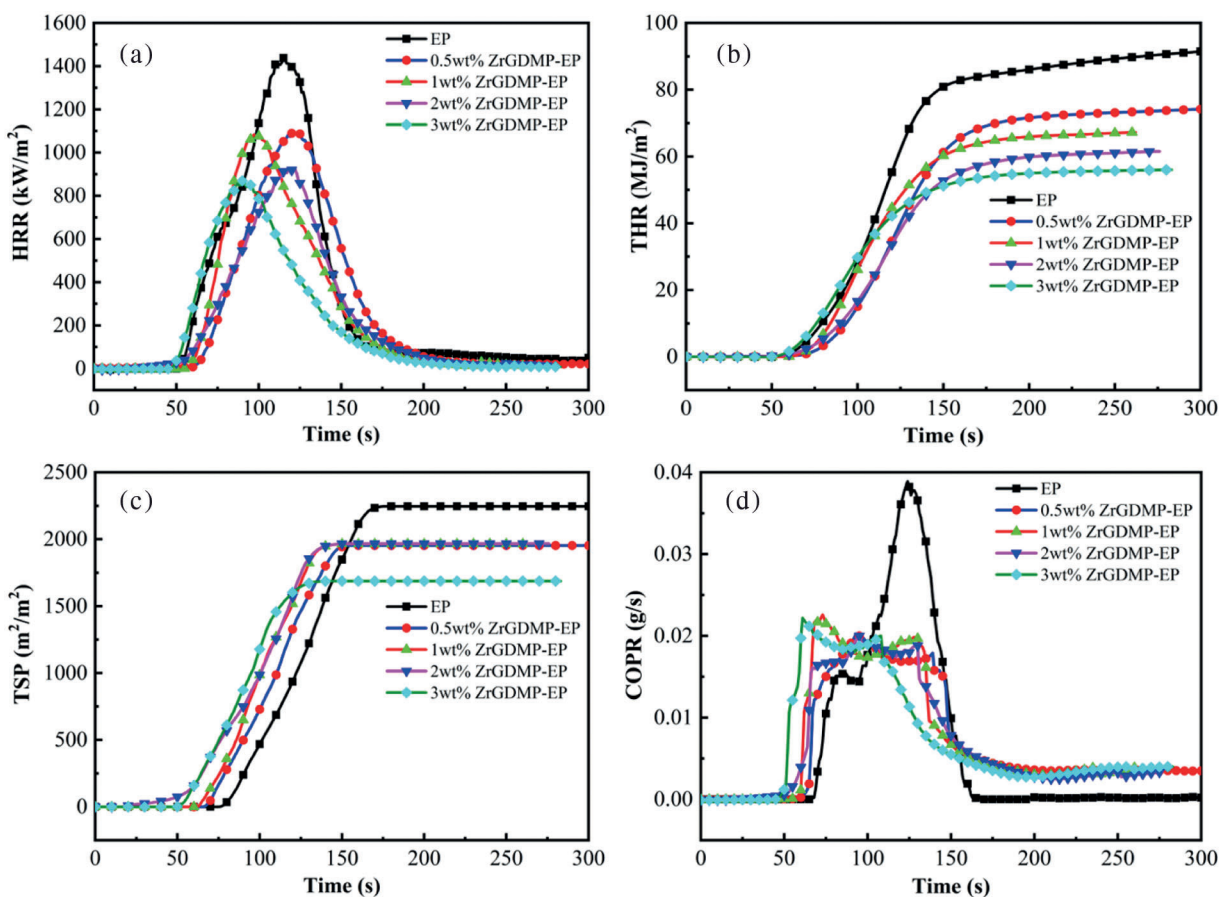


Figure 5: (a) HRR, (b) THR, (c) TSP and (d) COPR curves of EP and ZrGDMP-EP composites

Table 3: Data of the cone calorimetry test and the LOI test of EP and ZrGDMP-EP composites

Sample	PHRR (kW/m ²)	THR (MJ/m ²)	TSR (m ² /m ²)	CO production rate (g/s)	LOI (%)
EP	1438 ± 62	93.1 ± 3.8	2246 ± 110	0.039 ± 0.003	25.0 ± 0.5
0.5wt% ZrGDMP-EP	1100 ± 53	73.8 ± 2.7	1952 ± 82	0.020 ± 0.001	26.0 ± 0.5
1wt% ZrGDMP-EP	1038 ± 42	66.3 ± 2.3	1959 ± 97	0.023 ± 0.002	27.0 ± 0.5
2wt% ZrGDMP-EP	926 ± 46	60.4 ± 1.7	1892 ± 85	0.020 ± 0.001	27.5 ± 0.5
3wt% ZrGDMP-EP	869 ± 37	55.7 ± 1.9	1686 ± 75	0.022 ± 0.002	28.0 ± 0.5

The digital photos of the char residues of pure EP and ZrGDMP-EP composites after the cone calorimeter test are shown in Fig. 6. For pure EP, there was very little char residue left and the char residue was relatively loose with a lot of holes, while after the addition of ZrGDMP, the char residue of ZrGDMP-EP was thicker and compact. From the side picture of char residue, it was obvious that the height of the char residue increased gradually, and the height of the char residue of 3wt% ZrGDMP-EP reached 4 cm, indicating that ZrGDMP can promote char formation of EP. Moreover, char residue can serve as a physical barrier to isolate oxygen as well as heat and protect the internal substances of epoxy resin from further combustion. The combustible volatile gases produced during combustion were prevented into the flame layer to inhibit combustion. The char layer can also suppress the release of toxic gases such as smoke particles and CO, and had the effect of smoke suppression and toxicity reduction [28]. Thus, ZrGDMP can endow EP with much better fire-resistant performance.

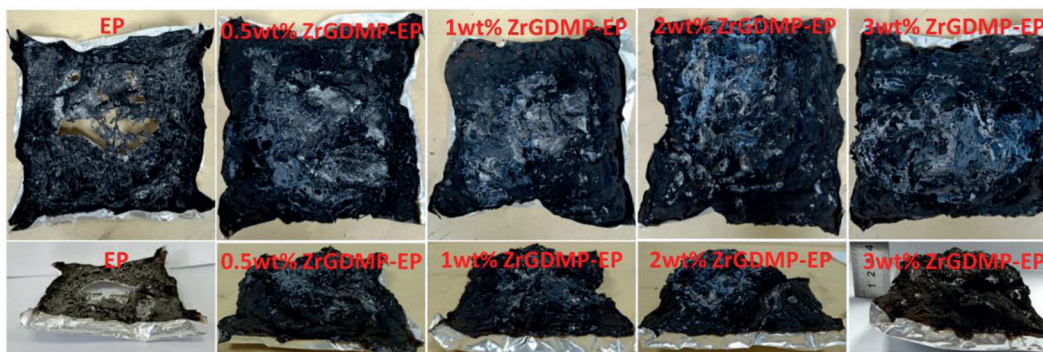


Figure 6: The digital photos of the char residues of pure EP and EP composites

The Raman spectra of the char residues of pure EP and ZrGDMP-EP composites are displayed in Fig. 7. The Raman spectrum of epoxy resin composites was similar to that of pure EP, which once again proved that the introduction of ZrGDMP did not change the combustion behavior of EP resin. There were two typical peaks at 1351 and 1590 cm^{-1} in the Raman spectra of char residue, which were allocated to the D band and G band, respectively. The ratio of peak area of these two peaks (I_D/I_G) can be used to compare and assess the graphitization degree of the char residues [29]. The lower the I_D/I_G value, the higher the graphitization degree of char residue. The I_D/I_G values of ZrGDMP-EP composites with different ZrGDMP content were 2.793, 2.787, 2.706 and 2.611, respectively, which was lower than that of pure EP (2.960). The I_D/I_G value decreased with the increase of ZrGDMP content, indicating that ZrGDMP can promote the formation of the char layer with a higher graphitization degree and better heat resistance.

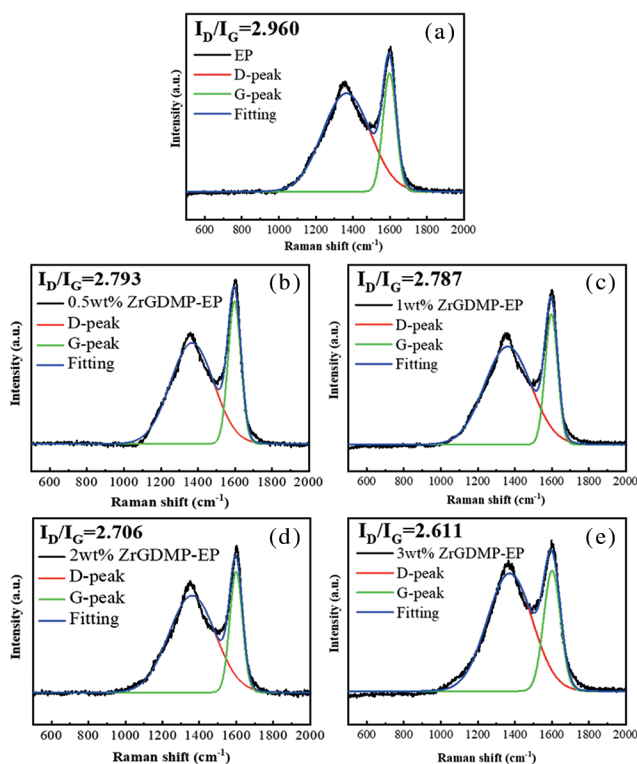


Figure 7: Raman spectra of the char residues of (a) EP (b) 0.5wt% ZrGDMP-EP (c) 1wt% ZrGDMP-EP (d) 2wt% ZrGDMP-EP (e) 3wt% ZrGDMP-EP

The SEM images of the char residue of EP and epoxy composites are shown in Fig. 8. The char residue of pure EP showed many voids and crack on the surface, while the surface of the char residue of ZrGDMP-EP composites was denser with no obvious cracks or just some individual small cracks, which was consistent with the results of digital photos of char residues. The addition of ZrGDMP can promote the formation of a dense and compact char layer which served as a physical barrier to protect the interior EP matrix.

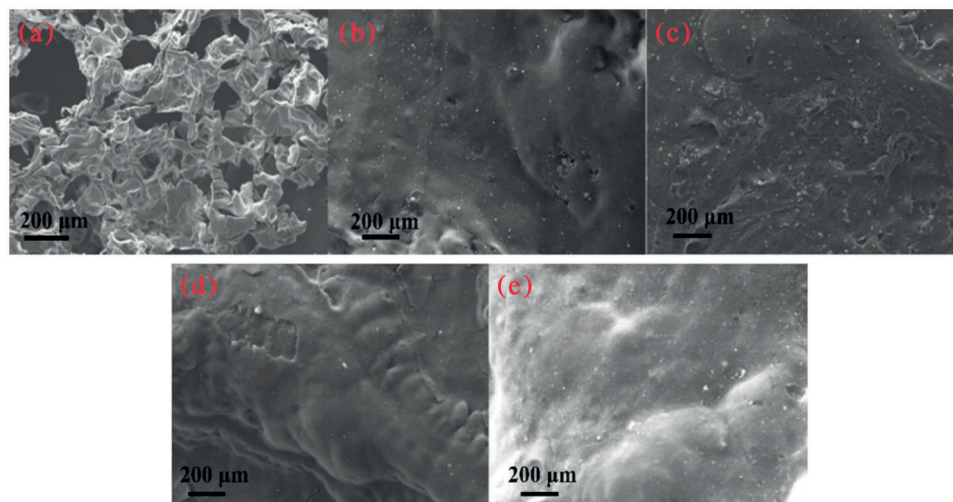


Figure 8: SEM images of the char residues of (a) EP (b) 0.5wt% ZrGDMP-EP (c) 1wt% ZrGDMP-EP (d) 2wt% ZrGDMP-EP (e) 3wt% ZrGDMP-EP

The thermal degradation gaseous products of EP and ZrGDMP-EP were investigated by TG-FTIR (Fig. 9). Some typical flammable volatile products were identified, including unsaturated hydrocarbons (3015 cm^{-1}), saturated hydrocarbons (2974 cm^{-1}), aromatic compounds (1508 cm^{-1}) and ethers (1174 cm^{-1}) [30,31]. The absorbance intensity curves of several representative volatile products are displayed in Fig. 10. Compared with pure EP, almost all the intensity of characteristic volatile products of 3wt% ZrGDMP-EP was significantly decreased, implying the less release of these volatile gases. Because most of these volatile products were flammable, the significant reduction of volatile products meant that the release of combustible gases was significantly reduced, resulting in the lower PHRR and THR values of 3wt% ZrGDMP-EP composites. According to the above various analysis results, possible flame retardant and smoke suppression mechanisms were proposed as below: thanks to weak Bronsted acid sites and strong Lewis acid sites on the layer, and the synergistic flame retardant effect of phosphorus and nitrogen, ZrGDMP can promote char formation and form a protective char layer, which can not only serve as a physical barrier to isolate oxygen and inhibit the release of smoke and toxic gases like CO but also protect the internal matrix from burning [32,33].

3.4 Mechanical Property

Fig. 11 shows the stress-strain curve of pure EP and ZrGDMP-EP composites. The detailed data are summarized in Table 4. The toughness of EP was relatively poor, whereas the addition of ZrGDMP can greatly enhance the toughness and strength of epoxy composites with a significant increase of the tensile strength as well as the elongation at break. Compared with pure EP, the tensile strength of 3wt% ZrGDMP-EP composites increased from 33.3 to 57.7 MPa and the elongation at break increased from 3.6% to 5.7%. Furthermore, the impact test of EP and its composites was carried out to further investigate the mechanical property of epoxy composites. The impact strength of pure EP was only 16.0 kJ/m^2 , while the impact strength of 0.5wt% ZrGDMP-EP was increased by 14.4% to 18.3 kJ/m^2 . The toughening effect of

ZrGDMP was mainly contributed to the that the small organic molecules on ZrGDMP improved the interfacial compatibility between ZrGDMP and EP matrix so that ZrGDMP molecules can be uniformly dispersed in the EP matrix, thus improving the strength and toughness of ZrGDMP/EP composites.

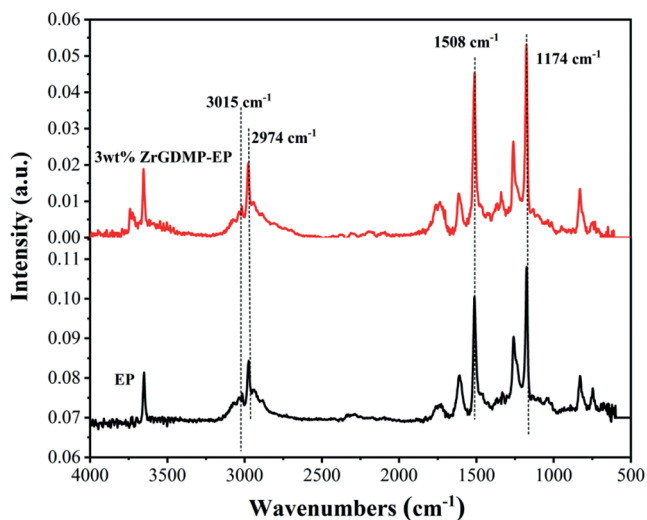


Figure 9: FTIR spectra of pure EP and 3wt% ZrGDMP-EP composites at the maximum degradation rate

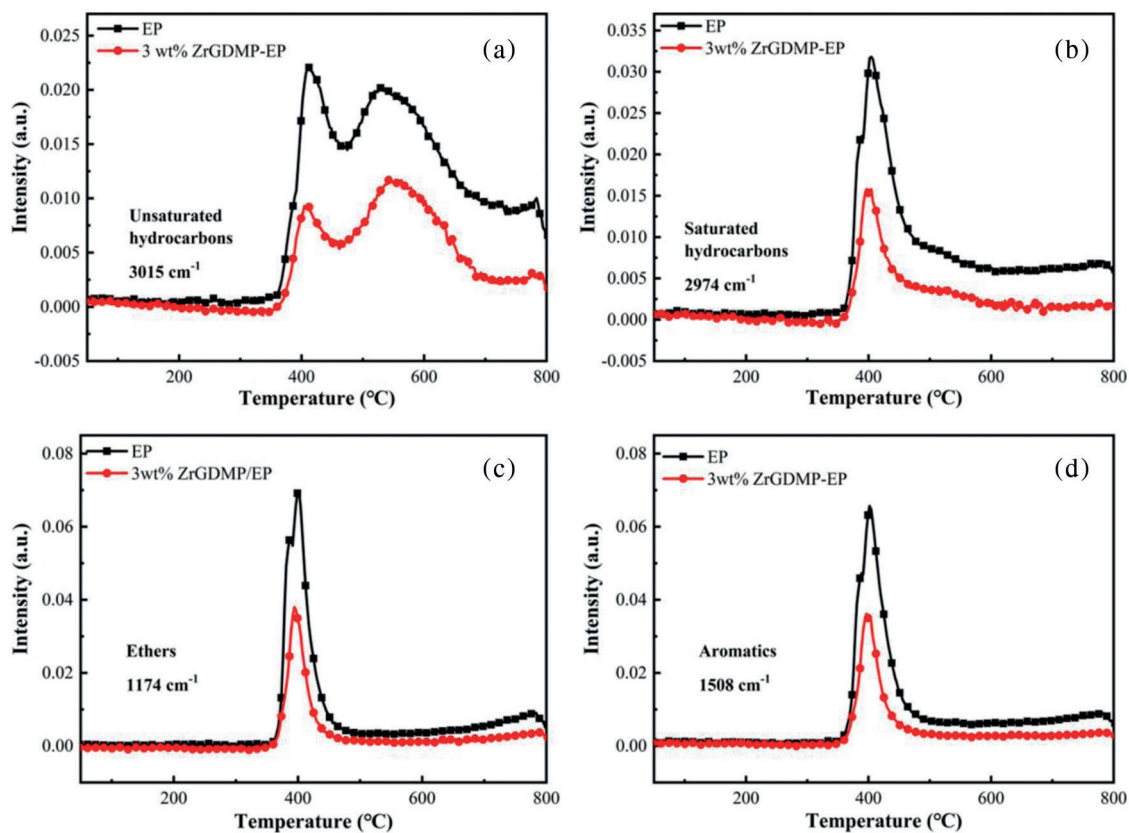


Figure 10: The plots of the absorbance intensity of typical volatile products as a function of temperature for pure EP and 3wt% ZrGDMP-EP composites

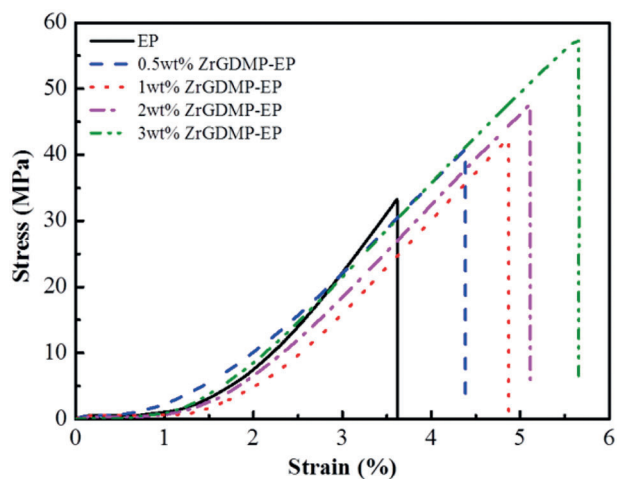


Figure 11: Stress-strain curves of pure EP and ZrGDMP-EP composites

Table 4: Tensile property and impact strength of pure epoxy and ZrGDMP/EP composites

Sample	Impact strength (kJ/m ²)	Tensile strength (MPa)	Elongation at break (%)
EP	16.0 ± 1.2	33.3 ± 1.3	3.6 ± 1.2
0.5wt% ZrGDMP-EP	18.3 ± 0.8	40.8 ± 0.7	4.4 ± 1.0
1wt% ZrGDMP-EP	21.0 ± 1.0	42.4 ± 1.1	4.9 ± 1.2
2wt% ZrGDMP-EP	23.1 ± 0.9	47.6 ± 1.2	5.1 ± 0.8
3wt% ZrGDMP-EP	24.8 ± 1.1	57.7 ± 0.9	5.7 ± 1.0

SEM images of fractured section of EP and 3wt% ZrGDMP-EP composites are presented in Fig. 12, as well as the elemental mapping of a section of 3wt% ZrGDMP-EP composites. It was observed that ZrGDMP nanoparticles were relatively uniformly dispersed in the EP matrix from the elemental mapping. The section of pure EP was smooth, indicating that EP material was a typical brittle rupture. Different from pure EP, the section surface of 3wt% ZrGDMP-EP composite was relatively rough with many folds and protuberances, showing that the introduction of ZrGDMP can hinder crack propagation and reinforce the mechanical properties of EP composites. Moreover, the interface compatibility between ZrGDMP and EP matrix was excellent, and the well-dispersed ZrGDMP nanoparticles produced a stress concentration effect during EP curing, which reduced the internal stress of the material.

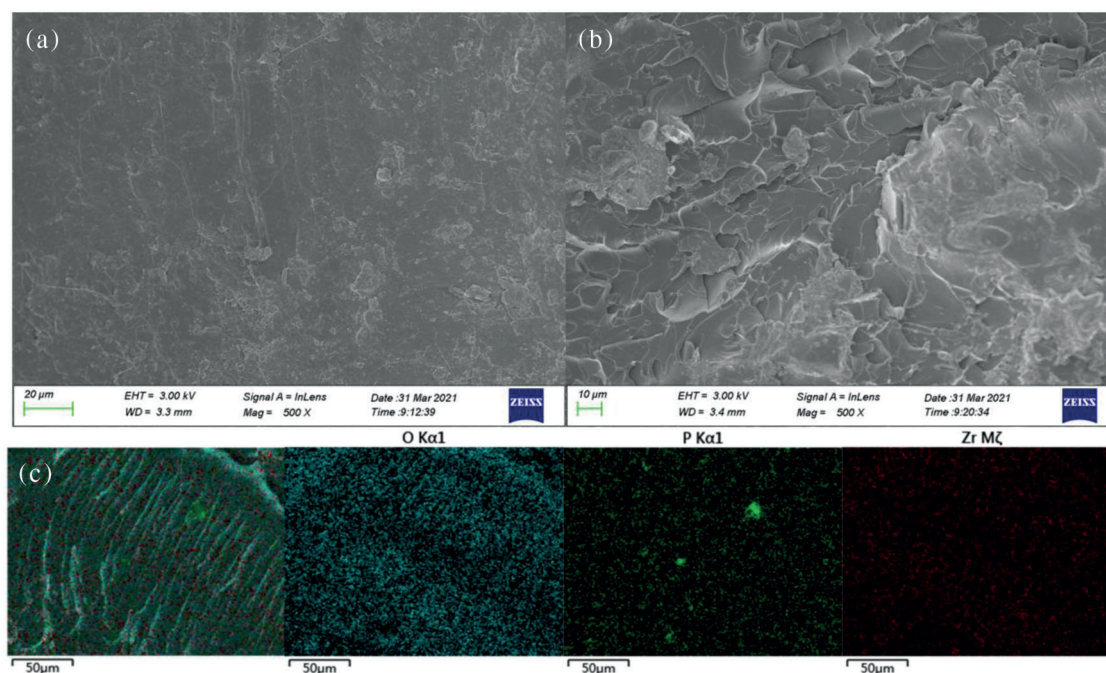


Figure 12: SEM images of fractured section of (a) EP; (b) 3wt% ZrGDMP-EP and (c) elemental mapping of fractured section of 3wt% ZrGDMP-EP composites

4 Conclusion

In conclusion, we prepared a new organic phosphonic acid N-bis(phosphomethyl) glycine (GDMP) by Mannich reaction with diphosphonic acid (glycine) and then synthesized a novel layered zirconium phosphonate (ZrGDMP) by using GDMP and zirconium phosphonate (ZrP) as reactants. Its flame retardant, smoke suppression, strengthening and toughening effects on the epoxy matrix were investigated and evaluated. The LOI value of ZrGDMP-EP increased slightly with the increase of ZrGDMP content. The PHRR of 3wt% ZrGDMP-EP was only 869 kW/m^2 . Similarly, the THR of 3wt% ZrGDMP-EP was reduced by 40.2% to 55.7 MJ/m^2 . The TSP and peak CO production rate significantly decreased as well. It was confirmed that ZrGDMP had significant flame retardant and smoke suppression effects on epoxy resin, which was contributed to the synergistic flame retardant effect of phosphorus and nitrogen, and the catalytic charring effect during combustion, thus reducing the risk of the conflagration of polymer materials. The toughness of EP was poor, whereas the addition of ZrGDMP can significantly reinforce the toughness and strength of EP composites with the higher tensile strength and elongation at break. The impact strength of 3wt% ZrGDMP-EP reached 24.8 kJ/m^2 , which was increased by 55%. Tensile and impact tests showed that the addition of ZrGDMP can significantly improve the toughness and strength of EP., which was mainly due to the outstanding interface compatibility between ZrGDMP and EP matrix so that ZrGDMP molecules can be well dispersed in the EP matrix, thus effectively improving the strength and toughness of epoxy composites.

Funding Statement: The authors acknowledged the financial support from the National Natural Science Foundation of China (Grant Nos. 22075265, 51991352) and the Youth Innovation Promotion Association of the Chinese Academy of Sciences (Grant Nos. 2021459).

Conflicts of Interest: The authors declare that they have no conflicts of interest to report regarding the present study.

References

1. Mohan, P. (2013). A critical review: The modification, properties, and applications of epoxy resins. *Polymer-Plastics Technology and Engineering*, 52(2), 107–125. DOI 10.1080/03602559.2012.727057.
2. Kumar, S., Samal, S. K., Mohanty, S., Nayak, S. K. (2018). Recent development of biobased epoxy resins: A review. *Polymer-Plastics Technology and Engineering*, 57(3), 133–155. DOI 10.1080/03602559.2016.1253742.
3. Unnikrishnan, K. P., Thachil, E. T. (2008). Synthesis and characterization of cardanol-based epoxy systems. *Designed Monomers and Polymers*, 11(6), 593–607. DOI 10.1163/156855508X363870.
4. Wang, X., Hu, Y., Song, L., Xing, W., Lu, H. et al. (2010). Flame retardancy and thermal degradation mechanism of epoxy resin composites based on a DOPO substituted organophosphorus oligomer. *Polymer*, 51(11), 2435–2445. DOI 10.1016/j.polymer.2010.03.053.
5. Guo, W., Zhao, Y., Wang, X., Cai, W., Wang, J. et al. (2020). Multifunctional epoxy composites with highly flame retardant and effective electromagnetic interference shielding performances. *Composites Part B: Engineering*, 192, 107990. DOI 10.1016/j.compositesb.2020.107990.
6. Mauerer, O. (2005). New reactive, halogen-free flame retardant system for epoxy resins. *Polymer Degradation and Stability*, 88(1), 70–73. DOI 10.1016/j.polymdegradstab.2004.01.027.
7. Mercado, L. A., Galia, M., Reina, J. A. (2006). Silicon-containing flame retardant epoxy resins: Synthesis, characterization and properties. *Polymer Degradation and Stability*, 91(11), 2588–2594. DOI 10.1016/j.polymdegradstab.2006.05.007.
8. Yang, P., Xia, T., Ghosh, S., Wang, J. C., Rawson, S. D. et al. (2021). Realization of 3D epoxy resin/Ti₃C₂T_x MXene aerogel composites for low-voltage electrothermal heating. *2D Materials*, 8(2), 025022. DOI 10.1088/2053-1583/Abda0f.
9. Wu, H., Cheng, L., Liu, C. B., Lan, X. J., Zhao, H. C. (2021). Engineering the interface in graphene oxide/epoxy composites using bio-based epoxy-graphene oxide nanomaterial to achieve superior anticorrosion performance. *Journal of Colloid and Interface Science*, 587(1), 755–766. DOI 10.1016/j.jcis.2020.11.035.
10. Fu, X. L., Wang, X., Xing, W., Zhang, P., Song, L. et al. (2018). Two-dimensional cardanol-derived zirconium phosphate hybrid as flame retardant and smoke suppressant for epoxy resin. *Polymer Degradation and Stability*, 151, 172–180. DOI 10.1016/j.polymdegradstab.2018.03.006.
11. Sen, A. K., Kumar, S. (2010). Coir-fiber-based fire retardant nano filler for epoxy composites. *Journal of Thermal Analysis and Calorimetry*, 101(1), 265–271. DOI 10.1007/s10973-009-0637-8.
12. Gerard, C., Fontaine, G., Bourbigot, S. (2010). New trends in reaction and resistance to fire of fire-retardant epoxies. *Materials*, 3(8), 4476–4499. DOI 10.3390/ma3084476.
13. Baby, A., Tretsiakova-McNally, S., Arun, M., Joseph, P., Zhang, J. P. (2020). Reactive and additive modifications of styrenic polymers with phosphorus-containing compounds and their effects on fire retardance. *Molecules*, 25(17), 3779. DOI 10.3390/molecules25173779.
14. Wu, Q., Miao, W. S., Zhang, Y. D., Gao, H. J., Hui, D. (2020). Mechanical properties of nanomaterials: A review. *Nanotechnology Reviews*, 9(1), 259–273. DOI 10.1515/ntrev-2020-0021.
15. Hajipour, A. R., Karimi, H. (2014). Synthesis and characterization of hexagonal zirconium phosphate nanoparticles. *Materials Letters*, 116, 356–358. DOI 10.1016/j.matlet.2013.11.049.
16. Chen, M. Y., Xia, J., Li, H., Zhao, X. G., Peng, Q. P. et al. (2021). A cationic Ru(II) complex intercalated into zirconium phosphate layers catalyzes selective hydrogenation via heterolytic hydrogen activation. *Chemcatchem*, 13(17), 3801–3814. DOI 10.1002/cctc.202100599.
17. Xu, L. F., Lei, C. H., Xu, R. J., Zhang, X. Q., Xu, J. B. (2018). Intumescent flame retardant of polypropylene system with enhanced thermal properties and flame retardancy based on alpha-zirconium phosphate composite particles. *Polymer Bulletin*, 75(6), 2707–2727. DOI 10.1007/s00289-017-2177-x.
18. Sun, H. Y., Fang, Z. Q., Li, T., Lei, F., Jiang, F. et al. (2019). Enhanced mechanical and tribological performance of PA66 nanocomposites containing 2D layered alpha-zirconium phosphate nanoplatelets with different sizes. *Advanced Composites and Hybrid Materials*, 2(3), 407–422. DOI 10.1007/s42114-019-00100-z.
19. Prado, L. A. S. D., Wittich, H., Schulte, K., Goerigk, G., Garamus, V. M. et al. (2004). Anomalous small-angle X-ray scattering characterization of composites based on sulfonated poly(ether ether ketone), zirconium phosphates,

- and zirconium oxide. *Journal of Polymer Science Part B–Polymer Physics*, 42(3), 567–575. DOI 10.1002/(ISSN) 1099-0488.
20. Melanova, K., Benes, L., Zima, V., Trchova, M., Stejskal, J. (2020). Polyaniline-zirconium phosphonate composites: Thermal stability and spectroscopic study. *Journal of Physics and Chemistry of Solids*, 147, 109634. DOI 10.1016/j.jpcs.2020.109634.
 21. Veliscek-Carolan, J., Rawal, A., Oldfield, D. T., Thorogood, G. J., Bedford, N. M. (2020). Nanoporous zirconium phosphonate materials with enhanced chemical and thermal stability for sorbent applications. *ACS Applied Nano Materials*, 3(4), 3717–3729. DOI 10.1021/acsnm.0c00405.
 22. Pica, M., Donnadio, A., Casciola, M. (2018). From microcrystalline to nanosized alpha-zirconium phosphate: Synthetic approaches and applications of an old material with a bright future. *Coordination Chemistry Reviews*, 374, 218–235. DOI 10.1016/j.ccr.2018.07.002.
 23. Pica, M., Donnadio, A., Mariangeloni, G., Zuccaccia, C., Casciola, M. (2016). A combined strategy for the synthesis of double functionalized alpha-zirconium phosphate organic derivatives. *New Journal of Chemistry*, 40(10), 8390–8396. DOI 10.1039/C6NJ01506A.
 24. Nie, L., Liu, C. H., Liu, L., Jiang, T., Hong, J. et al. (2015). Study of the thermal stability and flame retardant properties of graphene oxide-decorated zirconium organophosphate based on polypropylene nanocomposites. *RSC Advances*, 5(112), 92318–92327. DOI 10.1039/C5RA13850G.
 25. Zhang, Q., Liu, H., Li, X., Xu, R., Zhong, J. et al. (2016). Synthesis and characterization of polybenzimidazole/alpha-zirconium phosphate composites as proton exchange membrane. *Polymer Engineering and Science*, 56(6), 622–628. DOI 10.1002/pen.24287.
 26. Burnell, V. A., Readman, J. E., Tang, C. C., Parker, J. E., Thompson, S. P. et al. (2010). Synthesis and structural characterisation using Rietveld and pair distribution function analysis of layered mixed titanium-zirconium phosphates. *Journal of Solid State Chemistry*, 183(9), 2196–2204. DOI 10.1016/j.jssc.2010.07.028.
 27. Wang, X., Hu, Y., Song, L., Yang, H., Xing, W. et al. (2011). *In situ* polymerization of graphene nanosheets and polyurethane with enhanced mechanical and thermal properties. *Journal of Materials Chemistry*, 21(12), 4222–4227. DOI 10.1039/c0jm03710a.
 28. Zhang, J. T., Wu, W. Q., Lv, Y., Guo, C. L., Xu, Y. T. et al. (2021). Grafting multi-elements hybrid polymer brushes on graphene oxide for epoxy composite with excellent flame retardancy. *Journal of Applied Polymer Science*, 138(36), e50923. DOI 10.1002/app.50923.
 29. Niu, H., Nabipour, H., Wang, X., Song, L., Hu, Y. (2021). Phosphorus-free vanillin-derived intrinsically flame-retardant epoxy thermoset with extremely low heat release rate and smoke emission. *ACS Sustainable Chemistry & Engineering*, 9(15), 5268–5277. DOI 10.1021/acssuschemeng.0c08302.
 30. Huang, N. N., Wang, J. Q. (2009). A TGA-FTIR study on the effect of CaCO₃ on the thermal degradation of EBA copolymer. *Journal of Analytical and Applied Pyrolysis*, 84(2), 124–130. DOI 10.1016/j.jaap.2009.01.001.
 31. Ghosh, B., Chellappan, K. V., Urban, M. W. (2011). Self-healing inside a scratch of oxetane-substituted chitosan-polyurethane (OXE-CHI-PUR) networks. *Journal of Materials Chemistry*, 21(38), 14473–14486. DOI 10.1039/c1jm12321a.
 32. Lu, H. D., Wilkie, C. A., Ding, M., Song, L. (2011). Flammability performance of poly(vinyl alcohol) nanocomposites with zirconium phosphate and layered silicates. *Polymer Degradation and Stability*, 96(7), 1219–1224. DOI 10.1016/j.polymdegradstab.2011.04.014.
 33. Xu, L. F., Lei, C. H., Xu, R. J., Zhang, X. Q., Zhang, F. (2016). Functionalization of alpha-zirconium phosphate by polyphosphazene and its effect on the flame retardance of an intumescent flame retardant polypropylene system. *RSC Advances*, 6(81), 77545–77552. DOI 10.1039/C6RA15382H.